

Article

Growth and Genome Features of Non-O1/O139 *Vibrio cholerae* Isolated from Three Species of Common Freshwater Fish

Xinchi Qin ^{1,2}, Lianzhi Yang ^{1,2} , Yingwei Xu ^{1,2}, Lu Xie ³ , Yongjie Wang ^{1,2}  and Lanming Chen ^{1,2,*}

¹ Key Laboratory of Quality and Safety Risk Assessment for Aquatic Products on Storage and Preservation (Shanghai), Ministry of Agriculture and Rural Affairs of China, Shanghai 201306, China

² College of Food Science and Technology, Shanghai Ocean University, Shanghai 201306, China

³ Shanghai-MOST Key Laboratory of Health and Disease Genomics, Institute for Genome and Bioinformatics, Shanghai Institute for Biomedical and Pharmaceutical Technologies, Shanghai 200032, China

* Correspondence: lmchen@shou.edu.cn

Abstract: *Vibrio cholerae* is the etiological agent of cholera in humans. The bacterium is frequently detected in aquatic products worldwide. However, the current literature on the genome evolution of *V. cholerae* of aquatic animal origins is limited. Here, we firstly characterized the growth and genome features of *V. cholerae* isolates with different resistance phenotypes from three species of common freshwater fish. The results revealed that the non-O1/O139 *V. cholerae* isolates ($n = 4$) were halophilic and grew optimally at 2% NaCl and pH 8.0. Their draft genome sequences were 3.89 Mb–4.15 Mb with an average GC content of 47.35–47.63%. Approximately 3366–3561 genes were predicted to encode proteins, but 14.9–17.3% of them were of an unknown function. A number of strain-specific genes ($n = 221$ –311) were found in the four *V. cholerae* isolates, 3 of which belonged to none of any of the known sequence types (STs). Several putative mobile genetic elements (MGEs) existed in the *V. cholerae* isolates, including genomic islands ($n = 4$ –9), prophages ($n = 0$ –3), integrons ($n = 1$ –1), and insertion sequences ($n = 0$ –3). Notably, CRISPR-Cas system arrays ($n = 2$ –10) were found in the *V. cholerae* genomes, whereby the potential immunity defense system could be active. Comparative genomic analyses also revealed many putative virulence-associated genes ($n = 106$ –122) and antibiotic resistance-related genes ($n = 6$ –9). Overall, the results of this study demonstrate the bacterial broader-spectrum growth traits and fill prior gaps in the genomes of *V. cholerae* originating from freshwater fish.

Keywords: *Vibrio cholerae*; genome evolution; mobile genetic elements; virulence; antibiotic resistance; aquatic animals



Citation: Qin, X.; Yang, L.; Xu, Y.; Xie, L.; Wang, Y.; Chen, L. Growth and Genome Features of Non-O1/O139 *Vibrio cholerae* Isolated from Three Species of Common Freshwater Fish. *Diversity* **2024**, *16*, 268. <https://doi.org/10.3390/d16050268>

Academic Editors: Tomasz Grenda, Karol Stasiak and Krzysztof Kwiatek

Received: 16 March 2024

Revised: 26 April 2024

Accepted: 27 April 2024

Published: 30 April 2024



Copyright: © 2024 by the authors. Licensee MDPI, Basel, Switzerland. This article is an open access article distributed under the terms and conditions of the Creative Commons Attribution (CC BY) license (<https://creativecommons.org/licenses/by/4.0/>).

1. Introduction

Vibrio cholerae is the etiological agent of cholera, a highly contagious diarrhea disease that affects millions of people worldwide each year [1]. Currently, outbreaks of cholera still occur, especially in regions where access to safe drinking water is limited [1]. For instance, in Mozambique, in the most recent outbreak, the first case of cholera was reported to the World Health Organization (WHO) from the Lago district in Niassa Province on 14 September 2022. Until 19 February 2023, a total of 5237 suspected cases and 37 deaths have been reported from 29 districts across six of the eleven Provinces in Mozambique (<https://www.who.int/emergencies/disease-outbreak-news>, accessed on 2 June 2023). In addition, the consumption of fish products contaminated by *V. cholerae* has also been linked to cholera outbreaks [2]. The cholerae toxin (CT) and toxin-coregulated pilus (TCP) are the primary virulence factors present in epidemic *V. cholerae* strains of serotypes O1 and O139 [3].

Antibiotic treatment can effectively shorten the duration of diarrhea and limit the spread of cholera. Nevertheless, the intensive use of antibiotics in health and agriculture sectors has exacerbated the resistance crisis. The emergence of multidrug-resistant (MDR)

pathogens is a global health issue, which leads to higher morbidity and mortality and more healthcare costs [4]. The MDR *V. cholerae* strains have emerged and rapidly spread worldwide, particularly in Africa in recent years [5,6]. For example, Taviani et al. [5] isolated *V. cholerae* strains ($n = 70$) from drinking water samples ($n = 91$) collected in Moamba, Mozambique, in 2008. They found that all the isolates were resistant to Ampicillin (AMP); 51% and 13% of the isolates were also resistant to streptomycin (STP) and gentamicin (GM); and 13% of the isolates exhibited MDR profiles, showing resistance to at least three antibiotics. Abioye et al. [6] isolated *V. cholerae* strains ($n = 34$) from some seafood in the Eastern Cape Province, South Africa, in 2022, and found that 65.71% of the strains had MDR phenotypes. Recently, Schmidt et al. [7] reported the antibiotic resistance of 24 environmental *V. cholerae* non-O1/O139 strains collected in Germany and other European countries between 2011 and 2021. They found that 42% of the isolates ($n = 24$) were resistant to meropenem (MEM), 16.7% to tetracycline (TET) and doxycycline (DOX), 12.5% to trimethoprimand, and 8% to piperacillin-tazobactam (TZP).

Resistance genes (RGs) may mainly be spread through horizontal gene transfer (HGT), which is arguably the most significant driving force of bacterial evolution [8]. This transfer could occur specifically through mobile genomic elements (MGEs), such as integrons (Ins), prophages, genomic islands (GIs), and insertion sequences (ISs) [9]. HGT significantly contributes to microbial adaptation to the environments and to the hosts [10]. In the past decades, sequencing technology has been rapidly advancing, e.g., single-molecule real-time sequencing, Oxford nanopore sequencing, single-cell sequencing, and multi-omics sequencing [11,12]. This facilitates the deciphering of the molecule mechanism underlying the MDR and pathogenesis of *V. cholerae* at the whole-genome level. A total of 1708 *V. cholerae* isolates have been sequenced so far (GenBank database, <https://www.ncbi.nlm.nih.gov/>, accessed on 18 June 2023). Of these, complete genome sequences of 112 *V. cholerae* isolates are available in genome databases. However, the current literature on genome features of *V. cholerae* strains in aquatic animals is limited, particularly from freshwater fish.

In our prior studies, we isolated and identified a number of *V. cholerae* strains from many species of aquatic animals and water environments [2,13–15]. In follow up to our previous work, in this study, we further investigated the growth and genome features of the *V. cholerae* isolates, which displayed different resistance phenotypes and originated from three species of common freshwater fish, including *Aristichthys nobilis*, *Ctenopharyngodon idellus*, and *Parabramis pekinensis*. The prevalence of *V. cholerae* in these fish species has been reported in our previous study [2]. The objectives of this study were the following: (1) to examine the growth of *V. cholerae* isolates ($n = 4$) under varying pH and NaCl circumstances; (2) to sequence whole genomes of the *V. cholerae* isolates and identify MGEs and virulence- and resistance-related genes; and (3) to investigate the phylogenetic relatedness of the *V. cholerae* isolates.

2. Materials and Methods

2.1. *V. cholerae* Isolates and Culture Conditions

V. cholerae 7-6-5 and *V. cholerae* L10-48, *V. cholerae* L1-1, and *V. cholerae* B5-86 isolates were isolated from *A. nobilis*, *C. idellus*, and *P. pekinensis*, respectively (Table S1), which were sampled in fish markets in Shanghai, China, in 2017–2019 [2,13]. The *V. cholerae* isolates were routinely incubated in Trypticase Soy Broth (TSB) (3% NaCl, pH 8.5) at 37 °C with shaking at 180 rpm [2,13–15], unless otherwise specified.

2.2. Growth of *V. cholerae* Isolates under Different pH and NaCl Conditions

The TSB was adjusted to different pH values (6.0, 6.5, 7.0, 7.5, 8.0, and 8.5) and NaCl concentrations (0.5%, 1%, 2%, 3%, 4%, and 5%), respectively [16]. Growth curves of *V. cholerae* isolates under the different pH (6.0–8.5) and NaCl concentrations (0.5–5%) were determined individually at 37 °C for 24 h using Multimode Microplate Reader (BioTek Instruments, Winooski, VT, USA).

2.3. Genome Sequencing, Assembly, and Annotation

The *V. cholerae* strains were cultured in the TSB (2% NaCl, pH 8.0) until reaching the mid-logarithmic growth phase (mid-LGP) at 37 °C. The bacterial cells were collected at $2700 \times g$ for 10 min at 4 °C. The genomic DNA was extracted using the TIANamp Bacteria DNA Kit (Tiangen Biochemical Technology Co., Ltd., Beijing, China) and analyzed [9,17–19].

The 16S rRNA gene of *V. cholerae* strains was individually amplified by the PCR assay, and the PCR products were purified, sequenced, and analyzed [9,17–19].

Genome sequences of the *V. cholerae* isolates were determined by Shanghai Majorbio Bio-Pharm Technology Co., Ltd. in Shanghai, China, using the Illumina HiSeq $\times 10$ platform (Illumina, San Diego, CA, USA). The average length of sequencing reads was 150 bp. Sequence quality control and assembly were performed using SOAPdenovo software (version 2.04) [20]. The coding sequences (CDSs), rRNA genes, and tRNA genes were predicted using Glimmer software (version 3.02) [21], Barrnap tool (<https://github.com/tseemann/barrnap>, accessed on 11 April 2021), and tRNAscan-SE (version 2.0) software [22], respectively.

Each gene in *V. cholerae* genomes was functionally assigned against the non-redundant protein database of the National Center for Biotechnology Information (NCBI, <http://www.ncbi.nlm.nih.gov>, accessed on 16 June 2023) and classified by assigning a Clusters of Orthologous Groups (COGs) number with 80% identity and 90% coverage at $E \leq 1 \times 10^{-5}$. If a CDS did not hit any known function, it was labeled as function unknown. The Virulence Factor Database (<http://www.mgc.ac.cn/VFs>, accessed on 16 June 2023), Antibiotic Resistance Gene Database (<http://arpcard.mcmaster.ca>, accessed on 16 June 2023), and BacMET database [23] were used to predict virulence-, antibiotic-, and heavy metal resistance-related genes, respectively.

2.4. Comparative Genome Analysis

GIs in each of the *V. cholerae* genomes were predicted using IslandPath-DIMOB and IslandViewer software (version 1.0) [24], while Prophages, Ins, and ISs were predicted using Phage_Finder software (version 2.3.0) [25], Integron_Finder software (version 2.0) [26], and Isfinder software (<https://www-is.biotoul.fr/search.php>, accessed on 20 May 2023) [27], respectively. The clustered regularly interspaced short palindromic repeats (CRISPR)–Cas arrays were predicted using Mincd software (version 3) and CRISPRtyper (<https://cctyper.crispr.dk/#/submit>, accessed on 11 April 2021) [28].

Orthologous genes in each of *V. cholerae* genomes were predicted using OrthoMCL software (version 14-137) [29], with their encoding proteins having at least more than 60% amino acid identity and 80% sequence coverage. Proteins with less than 30% identity or no matches were classified as strain-specific genes at a significance level of $E \leq 1 \times 10^{-5}$ [9,17–19].

2.5. Multilocus Sequence Typing (MLST) Analysis

The MLST analysis of each of the *V. cholerae* isolates was performed against the PubMLST database, on the basis of the conserved *gyrB*, *mdh*, *pntA*, *metE*, *pyrC*, *adk*, and *purM* genes in *V. cholerae* [30].

2.6. Phylogenetic Tree Construction

The phylogenetic tree of 71 *V. cholerae* isolates was constructed using the maximum likelihood approach [9,17–19]. The cutoff threshold for bootstrap values was set above 50%. Complete genome sequences of the 69 *V. cholerae* isolates were downloaded from the GenBank database (Table S2).

2.7. Antibiotic and Heavy Metal Resistance Assays

Antibiotic resistance of *V. cholerae* isolates was examined using the standard disco diffusion method approved by the Clinical and Laboratory Standards Institute (CLSI, M100-S23, 2018), Malvern, PA, USA. The heavy metal tolerance of *V. cholerae* isolates was also examined following the broth dilution testing (microdilution, CLSI) [2,13–15].

The same chemicals and quality control strains were used as described in our recent reports [2,13–15].

The SPSS software (version 22, IBM, Armonk, NY, USA) was utilized to analyze the collected data. All tests were performed in triplicate.

3. Results and Discussion

3.1. Growth Profiles of the Four *V. cholerae* Isolates under Different pH and NaCl Conditions

V. cholerae 7-6-5 and L1-1, L10-48, and B5-86 isolates were isolated from *A. nobilis*, *C. idellus*, and *P. pekinensis*, respectively (Table S1). The strains were confirmed by 16S rRNA gene sequencing and analysis (Table S1).

Human acidic stomach pH is close to 2.0, and reaches 6.0 after eating food, while intestinal pH is close to 8.0. This challenges the survival of *V. cholerae*, which forms colonies in the intestinal tract and causes severe diarrhea disease and even death [3]. In our prior study, we observed that the growth of *V. cholerae* isolates was highly inhibited below pH 6.0. Therefore, we examined the growth traits of the four *V. cholerae* isolates of aquatic animal origins under different pH conditions (pH 6.0–8.5). As shown in Figure 1A–D, different growth profiles were observed among the *V. cholerae* isolates incubated in the TSB (3% NaCl) at 37 °C. For instance, the acidic condition (pH 6.0) slightly repressed the growth of *V. cholerae* 7-6-5. This isolate was capable of growing vigorously in a broader spectrum of pH conditions (pH 6.5–8.5) but showed the maximum biomass with an OD₆₀₀ value of 1.332 at pH 8.0 (Figure 1A). Conversely, the *V. cholerae* L1-1 isolate was the most sensible to the acidic conditions among the test *V. cholerae* strains, as the growth of *V. cholerae* L1-1 was obviously inhibited at pH 6.0–7.5 (Figure 1C).

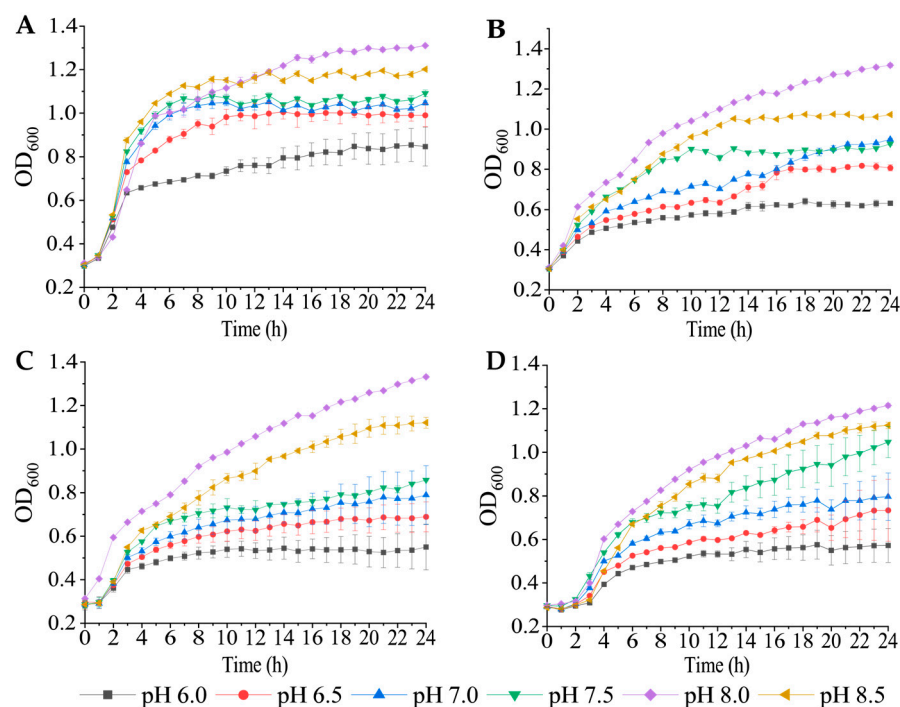


Figure 1. Growth profiles of the four *V. cholerae* isolates under different pH conditions. The isolates were incubated in the TSB (3% NaCl) at 37 °C. (A–D): *V. cholerae* 7-6-5, L10-48, L1-1, and B5-86 isolates, respectively.

Although the four *V. cholerae* isolates were isolated from *A. nobilis*, *C. idellus*, and *P. pekinensis*, which were aquacultured in a freshwater environment, distinct growth profiles of the *V. cholerae* strains were observed under different NaCl concentrations (0.5–5%), when incubated in the TSB (pH 8.0) at 37 °C (Figure 2A–D). For example, *V. cholerae* 7-6-5 appeared to be the most adaptable to the lower NaCl concentrations (0.5–1.0%), under

which this isolate was able to reach the maximum biomass with OD₆₀₀ values of 0.725–0.796 (Figure 2A). Conversely, the growth of *V. cholerae* L10-48, L1-1, and B5-86 isolates was inhibited with 0.5–1.0% of NaCl (Figure 2B–D). All the strains grew well at 2–5% of NaCl, but the maximum biomass was at 2% NaCl, which was lower than the routine culture condition (3% NaCl) for *V. cholerae* strains [2].

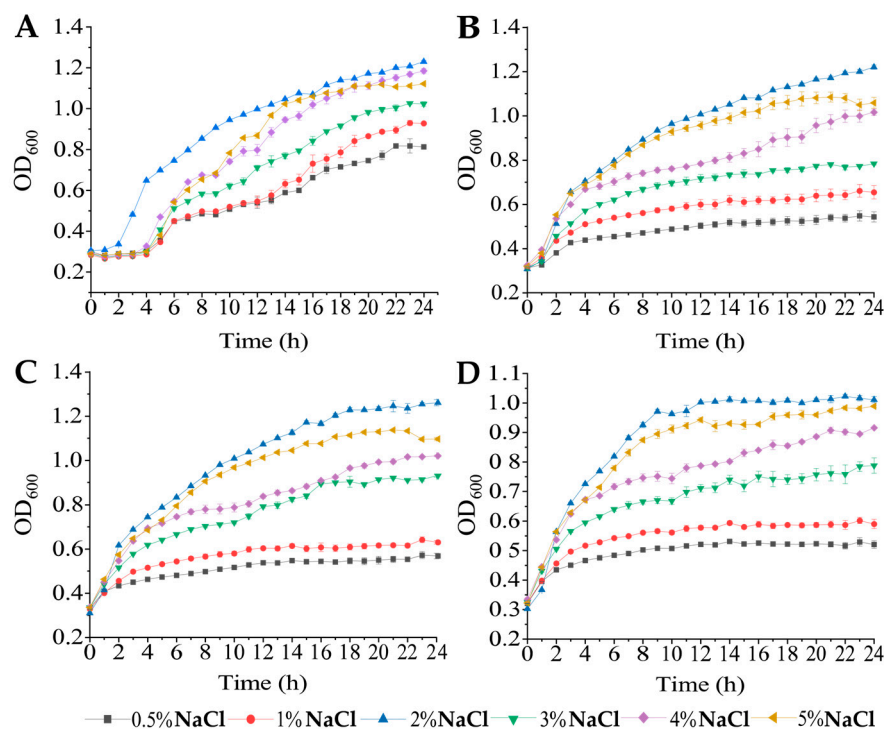


Figure 2. Growth profiles of the four *V. cholerae* isolates under different concentrations of NaCl. The isolates were incubated in the TSB (pH 8.0) at 37 °C. (A–D): *V. cholerae* 7-6-5, L10-48, L1-1, and B5-86 isolates, respectively.

Taken together, these results indicated that the four *V. cholerae* isolates that originated from the common freshwater fish were halophilic and grew optimally at pH 8.0 and 2% NaCl. *V. cholerae* 7-6-5 was the most fit to the broader spectrum of pH (6.5–8.5) and NaCl (0.5–3.0%) circumstances among the test isolates.

3.2. Genome Features of the Four *V. cholerae* Isolates from the Common Freshwater Fish

In this study, the genome sequences of the four *V. cholerae* isolates were determined using the Illumina HiSeq × 10 sequencing platform. Approximately 61,043–102,056 clean and high-quality sequencing reads were obtained, and the sequence assembly yielded 49–175 scaffolds with an average sequencing depth of 288.0-fold to 321.14-fold. The assembled genome sizes of the four *V. cholerae* isolates were 3.89 Mb–4.15 Mb of two chromosomes, with an average GC content of 47.35–47.63% (Table 1, Figure 3), consistent with the other *V. cholerae* strains. For example, the reference genome of *V. cholerae* N16961 was 4.03 Mb with an average 47.3% G + C content [31]. In this study, approximately 3486–3659 genes were predicted to encode proteins, but 14.4–16.8% of which were of an unknown function that accounted for the largest proportion among the 24 catalogs in the COG database (Figure S1).

Table 1. Genome features of the four *V. cholerae* isolates from common freshwater fish.

Genome Feature	<i>V. cholerae</i> Isolate			
	7-6-5	L10-48	L1-1	B5-86
Genome size (bp)	3,886,208	4,145,566	4,032,220	3,942,938
G + C (%)	47.44	47.35	47.58	47.63
DNA Scaffold	175	80	79	49
Predicted gene	3500	3663	3570	3487
Protein coding gene	3404	3561	3476	3366
RNA gene	96	102	94	121
Genes assigned to COG	2981	3046	3010	2985
Genes with unknown function	519	617	560	502
GIs	4	9	6	4
Prophage gene cluster	0	2	3	1
Ins	1	1	1	1
ISs	0	3	1	2
CRISPR-Cas array	8	10	6	2
BioSample accession no.	SAMN37882014	SAMN37882015	SAMN37882016	SAMN37882017

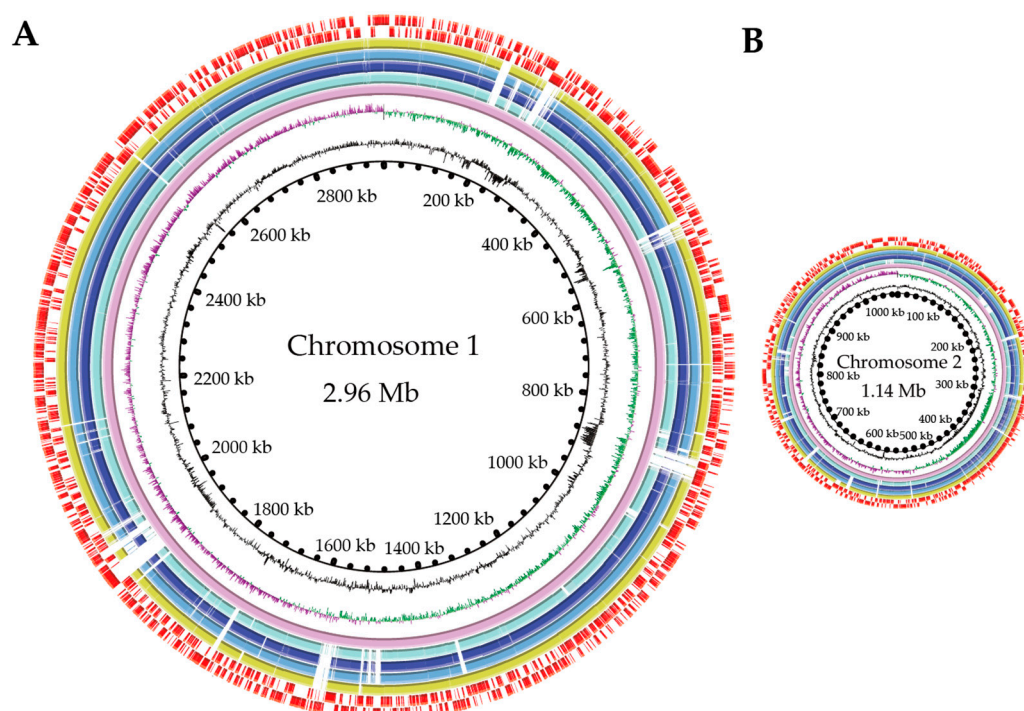


Figure 3. Genome circle maps of the four *V. cholerae* isolates from common freshwater fish. (A,B): represent the larger and smaller chromosomes, respectively. Circles from the inwards to outside: the GC content, GC-skew, the reference genome of *V. cholerae* N16961, and *V. cholerae* 7-6-5, L10-48, L1-1, and B5-86 genomes, respectively. The eighth and ninth circles (in red) represent CDSs on the positive and negative chains (inward and outward parts), respectively.

Comparative genomics analysis also revealed several MGEs in the four *V. cholerae* genomes, including the GIs ($n = 4-9$), prophage gene clusters ($n = 0-3$), Ins ($n = 1-1$), and ISs ($n = 0-3$), suggesting the potential HGT facilitated by the MGEs.

Additionally, the distribution of sequencing depth displayed a typical Poisson distribution (Figure S2), suggesting a lower proportion of repetitive DNA in the four *V. cholerae* genomes. On the other hand, a few repeats were observed at the end of scaffolds ($n = 3-7$, <1.3 Kb), suggesting that the un-assembled gaps between scaffolds were repetitive DNA (Table S3).

The draft genomes of the *V. cholerae* 7-6-5, L10-48, L1-1, and B5-86 isolates were deposited in the GenBank database under the bioSample accession numbers SAMN37882014, SAMN37882015, SAMN37882016, and SAMN37882017, respectively.

3.3. Putative MGEs in the Four *V. cholerae* Isolates from the Common Freshwater Fish

3.3.1. GIs

The GIs carry large foreign DNA fragments (~200 Kb) that facilitate the bacterial survival in the hosts and in the environments [17]. In this study, several GIs ($n = 4-9$) were identified in the four *V. cholerae* genomes (Figure S3, Table S4), among which *V. cholerae* L10-48 derived from *C. idellus* had the maximum number of GIs ($n = 9$, GIs 1-9). Nevertheless, the number of GIs was less than those ($n = 11$) identified in the genome of *V. cholerae* N16961 of serotype O1.

A total of 331 genes were predicted in the 23 GIs (1302 bp–37,045 bp) identified in the four *V. cholerae* genomes, which endowed the bacterium with additional biological functions, e.g., resistance, and substance metabolism. For instance, antibiotic resistance-related genes were found in some GIs, e.g., GI 3 (5770 bp) in *V. cholerae* 7-6-5 and GI 3 (12,834 bp) in *V. cholerae* B5-86. Phages-related genes were also found in some GIs in the *V. cholerae* genomes, e.g., GI 2 (8745 bp) in *V. cholerae* L10-48, GI 3 (5552 bp) in *V. cholerae* L1-1, and GI 2 (27,273 bp) in *V. cholerae* B5-86.

3.3.2. Prophages

Phages dominate the aquatic ecosystems on the Earth [32]. To the best of our knowledge, the current literature on prophages in *V. cholerae* genomes is rare.

In this study, six prophage gene clusters (9538 bp–42,593 bp) were identified in the *V. cholerae* L1-1, L10-48, and B5-86 genomes ($n = 1-3$), whereas none were found in *V. cholerae* 7-6-5. A total of 248 genes were predicted in the six prophages, which encoded phage structure proteins, e.g., the phage holin family proteins; phage tail, sheath, and assembly proteins; phage baseplate assembly proteins; and phage small head proteins. Notably, approximately 53.6% of the prophage genes coded for unknown proteins (Figure S4, Table S5).

The *V. cholerae* L1-1 genome contained three prophage gene clusters, which showed sequence similarity to *Escherichia*_phage_lys12581Vzw (38,198 bp, NCBI accession number: NC_049917), *Vibrio*_phage_VHML (42,593 bp, NCBI accession number: NC_004456), and *Vibrio*_phage_VCY_phi (9538 bp, NCBI accession number: NC_016162). *V. cholerae* L10-48 harbored two prophage gene clusters, showing sequence similarity to *Burkholderia*_cenocepacia_phage_BcepMa (24,437 bp, NCBI accession number: NC_005882) and *Escherichia*_phage_Arg0145 (42,272 bp, NCBI accession number: NC_049918). Additionally, only one *Escherichia*_converting_phage_Stx2a_F451 (40,712 bp, NCBI accession number: NC_049924) homologue was found in *V. cholerae* B5-86. Of note, the six identified prophages in the *V. cholerae* genomes were derived from three different genera, including *Burkholderia* cenocepacia, *Escherichia* spp., and *Vibrio* spp., indicating the possible phage transmission across these genera boundaries.

Additionally, one *Vibrio*_phage_CTX (13,121 bp, NCBI accession number: NC_015209) was identified in the *V. cholerae* N16961 genome, which encoded the CT and TCP, consistent with the previous report [31].

3.3.3. Ins

Mobile Ins were widespread in environments heavily influenced by human activity, with prolonged exposure to detergents, antibiotics, and heavy metals [33]. Ins are grouped into Type I, Type II, Type III, and super integrons, based on integrase genes (*intI1*, *intI2*, *intI3*, and *intI4*) [34].

In this study, each of the four *V. cholerae* genomes contained one complete In (2759–13,159 bp) (Figure S5, Table S6). For example, the identified In in the *V. cholerae* 7-6-5 genome encoded the IntI4 (*Vc* 7_6_5_1252) and QnrVC family quinolone resistance pentapeptide repeat protein (*Vc* 7_6_5_1250), suggesting that it was a super In. Notably, a

similar super In encoding the quinolone resistance protein was also found in the *V. cholerae* L1-1 and B5-86 genomes. The former also coded for the DUF4144 domain-containing proteins (*Vc L1_1_2144*), while the latter encoded the GNAT family *N*-acetyltransferase (*Vc B5_86_2255*) as well. One super In was found in the *V. cholerae* L10-48 genome, which encoded the IntI4, HNH endonuclease, and IS30 family transposase (*Vc L10_48_2217*, *Vc L10_48_2215*, and *Vc L10_48_2214*). Additionally, no Ins were identified in the *V. cholerae* N16961 genome.

3.3.4. ISs

ISs belonging to the IS3 and IS5 families play an important role in the evolution of antibiotic resistance and virulence in Gram-negative bacteria [35]. In this study, only a few ISs ($n = 1-3$, 620 bp–1551 bp) were identified in the *V. cholerae* L10-48, L1-1, and B5-86 genomes, whereas none were found in *V. cholerae* 7-6-5 (Table S7).

For instance, the *V. cholerae* L10-48 genome contained three ISs (IS001–IS003). The IS001 (1238 bp) coded for the ISAs1 family transposase (*Vc L10_48_1267*); IS002 (1045 bp) for the IS30 family transposase (*Vc L10_48_2214*); and IS003 (961 bp) for the IS5 family transposase (*Vc L10_48_1263*). However, none of the ISs carried antibiotic resistance- or virulence-related genes in the three *V. cholerae* genomes.

3.4. CRISPR-Cas System Arrays

The CRISPR-Cas system provides the host with an adaptive and hereditary immunity against exogenous nucleic acids [36]. In this study, the CRISPR-Cas system arrays ($n = 2-10$, 74 bp–4468 bp) were identified in all the four *V. cholerae* genomes (Figure S6).

For example, the *V. cholerae* L10-48 genome had the maximum number of CRISPR-Cas arrays ($n = 10$). Of these, the CRISPR 4 was the longest in size (2834 bp), with the maximum number of repetitive sequences ($n = 47$). In contrast, the *V. cholerae* B5-86 genome had the fewest CRISPR-Cas arrays ($n = 2$).

Remarkably, the genes encoding CRISPR-associated Cas proteins were identified in the *V. cholerae* L10-48 ($n = 5$), 7-6-5 ($n = 3$), and L1-1 ($n = 1$) genomes, whereas no such gene was found in *V. cholerae* B5-86. For instance, the *V. cholerae* L10-48 genome contained the *casA* (*Vc L10_48_3096*), *casB* (*Vc L10_48_3095*), *casC* (*Vc L10_48_3093*), *casD* (*Vc L10_48_3092*), and *casE* (*Vc L10_48_3094*) genes, while *V. cholerae* 7-6-5 contained three copies of the *cas6f* (*Vc 7_6_5_3049*, *Vc 7_6_5_2545*, and *Vc 7_6_5_0501*) genes. Only one *cas6f* (*Vc L1_1_0413*) gene was found in *V. cholerae* L1-1 (Table S8). The Cas is an endonuclease that can cleave foreign DNA [37]. These results suggested the potential active immunity defense systems in the *V. cholerae* isolates, which may have led to the fewer MGEs in the isolates. In contrast, in our recent study, we found many more MGEs present in *Klebsiella oxytoca* strains ($n = 8$) isolated from eight species of aquatic animals, particularly GIs ($n = 105$) and prophages ($n = 24$) [9]. Of note, although the CRISPR-Cas arrays were identified, the *cas* gene was absent from the *K. oxytoca* genomes, suggesting their inactive bacterial CRISPR-Cas systems [9]. Most recently, Wang et al. have successfully applied the Cas9-natural excision (NE) method to remove four representative MGEs, including plasmids, prophages, and GIs, from *Vibrio* strains [38], which provided the experimental evidence for the possible correlation between the Cas protein and MGEs. Interestingly, the *cas* gene appeared to be absent from *V. cholerae* N16961 as well.

3.5. Putative Virulence-Associated Genes in the Four *V. cholerae* Genomes

The genes encoding the CT and TCP were absent from the four *V. cholerae* genomes. The non-epidemic *V. cholerae* strains without the CT and TCP, referred to as non-O1/O139, can cause sporadic episodes of diarrhea and gastrointestinal infection [39,40]. Nevertheless, the Zonula occludens toxin gene (*zot*) was found in *V. cholerae* L1-1 and B5-86. *Zot* can increase the permeability of the small intestinal mucosa [41].

In addition, the genomes of *V. cholerae* 7-6-5, L1-1, L10-48, and B5-86 isolates contained the genes encoding the Type VI secretion system (T6SS) [42], the latter two of which

also encoded the Type III secretion system (T3SS) [43]. The four *V. cholerae* genomes also contained the genes encoding the virulence-related flagella, mannose hemagglutinin pili, and autoinducers (e.g., autoinducer-2, AI-2; and cholerae autoinducer-1, CAI-1) required for the biofilm formation in *V. cholerae*. The co-existence of the other virulence-related genes was found in the *V. cholerae* genomes as well (Table S9). For example, the *V. cholerae* 7-6-5 genome encoded the cell surface-expressed elongation factor EF-Tu (*Vc 7_6_5_2186*, *Vc 7_6_5_2235*, *Vc 7_6_5_3026*, and *Vc 7_6_5_3364*) [44], and lipid mediator receptors connected lipo-oligosaccharides (LOSs) (*Vc 7_6_5_0960*) [45]. The LOSs of *Histophilus somni* may act as an adhesin and an endotoxin that signals through toll-like receptor 4 and NF- κ B to cause inflammation in the host [45]. The RTX toxin genes (*Vc 7_6_5_2268*; *Vc 7_6_5_2265*; and *Vc 7_6_5_2266*) were also identified in *V. cholerae* 7-6-5, which was previously characterized by its ability to round human laryngeal epithelial (HEp-2) cells [46]. Two genes (*Vc 7_6_5_2990*; *Vc 7_6_5_2991*) involved in the *V. cholerae* cytolysin (VCC) were found in *V. cholerae* 7-6-5, which was among disparate pore-forming toxins [47].

Of note, *V. cholerae* B5-86 originating from *P. pekinensis* had the maximum number of virulence-related genes ($n = 122$), whereas *V. cholerae* L1-1 from *C. idellus* had the fewest ones ($n = 106$). These results suggested the potential risk of consuming the freshwater fish contaminated by these *V. cholerae* strains. In future research, the potential virulence of these *V. cholerae* strains should be further investigated at cell and animal mode levels.

3.6. Resistance-Associated Genes in the Four *V. cholerae* Genomes and Their Resistance Phenotypes

AMP is widely applied to treat foodborne bacterial infections. However, the treatment efficiency on the *Vibrio* infection has increasingly become ineffective, possibly due to the *crp* gene [48]. In this study, antibiotic resistance-related genes ($n = 6-9$), e.g., *crp*, *VarG*, *catB9*, *CARB-7*, *QnrVC4*, and *almG*, were identified in the four *V. cholerae* genomes (Table 2).

For example, the four *V. cholerae* genomes all carried the *crp* and *AlmG* genes. The former encoded a *crp* regulator in *Escherichia coli* by repressing the expression of the MdtEF multidrug efflux pump [48]. *AlmG* is a glycytransferase responsible for the polymyxin resistance in pandemic *V. cholerae* [49]. *V. cholerae* 7-6-5 also contained the *QnrVC4* and *VarG* genes. The former is an In-mediated quinolone resistance protein in *Aeromonas punctata* [50]. Lin et al. [51] reported that *VarG* of *V. cholerae* N16961 has β -lactamase activity against penicillins, cephalosporins and carbapenems. In this study, we found that *V. cholerae* L10-48 also contained the *catB9* and *CARB-7* genes responsible for the chloramphenicol and ampicillin resistance (*CARB-7*), respectively [52,53].

Table 2. The antimicrobial resistance-associated genes identified in the four *V. cholerae* genomes.

Antibiotic Agent	Resistance-Related Gene	<i>V. cholerae</i> Isolate	Reference
Fluoroquinolone	<i>crp</i>	7-6-5, L1-1, L10-48, B5-86	[48]
	<i>QnrVC4</i>	7-6-5, L1-1, B5-86	[50]
Chloramphenicol	<i>catB9</i>	L10-48	[52]
Carbapenem	<i>VarG</i>	7-6-5, B5-86	[51]
Polymyxin	<i>AlmG</i> , <i>ugd</i>	7-6-5, L1-1, L10-48, B5-86	[49,54]
beta-Lactam	<i>CARB-7</i>	L10-48	[53]
Nitroimidazole	<i>msbA</i>	7-6-5, L1-1, L10-48, B5-86	[55]
Streptogramin	<i>vatF</i>	7-6-5, L1-1, L10-48, B5-86	[56]

To verify the in silico predicted resistance genes, we examined the resistance phenotypes of the *V. cholerae* isolates experimentally, and the results are shown in Table S1. For example, *V. cholerae* 7-6-5 was resistant to antibiotics moxifloxacin (MXF) and rifampicin (RIF), as well as heavy metals Hg, Ni, Pb, and Zn; *V. cholerae* L10-48 was only resistant to AMP and STR; *V. cholerae* L1-1 solely tolerated Hg and Pb; and *V. cholerae* B5-86 was resistant to STR, Hg, Pb, and Zn (Table S1).

Based on the BacMET database, no heavy metal tolerance-related genes were identified in the *V. cholerae* genomes, which was not consistent with the heavy metal tolerance

phenotypes of *V. cholerae* 7-6-5, L1-1, and B5-86. We could not rule out the possibility that certain MDR efflux pumps are involved in the pumping out of heavy metals as well [57].

3.7. Strain-Specific Genes of the Four *V. cholerae* Isolates from the Common Freshwater Fish

A number of strain-specific genes ($n = 221$ – 311) were identified in the four *V. cholerae* isolates (Figure 4). *V. cholerae* 7-6-5 from *A. nobilis* harbored the highest number of strain-specific genes ($n = 311$), whereas *V. cholerae* B5-86 from *P. pekinensis* had the relative fewer ones ($n = 221$). Additionally, 2922 core genes were found in the four *V. cholerae* strains, which accounted for 65.6% of the pan genes ($n = 4457$) that were conserved in all the analyzed genomes. In addition, the genes of plasmid origins were also found in the four *V. cholerae* genomes. In future research, it will be interesting to sequence the plasmids extracted from the *V. cholerae* strains and decipher their function and evolution.

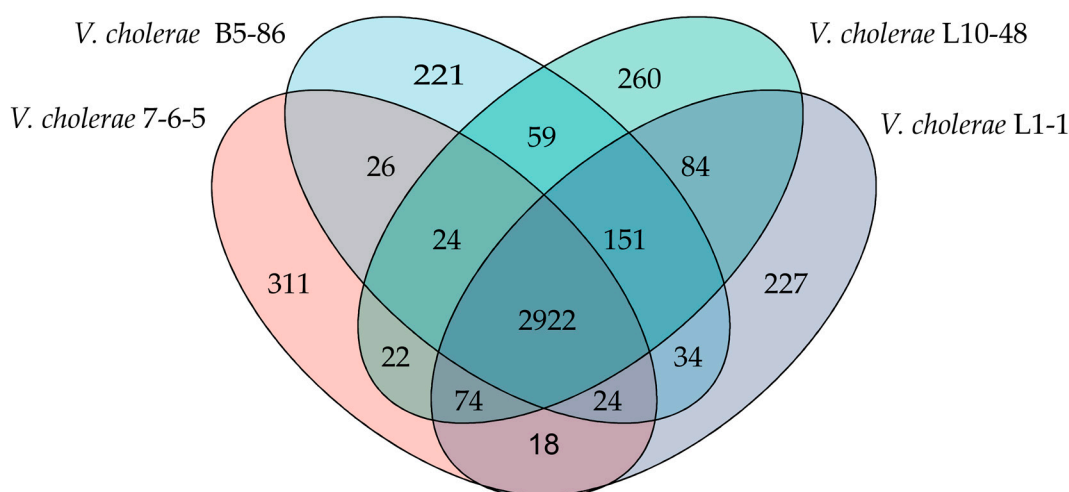


Figure 4. The Venn diagram shows the pan genes of the four *V. cholerae* strains from the freshwater fish. The central region represents the number of core genes, and each petal displays the number of specific genes for each strain.

3.8. MLST of the Four *V. cholerae* Isolates from the Common Freshwater Fish

In this study, the MLST analysis against the PubMLST database revealed that *V. cholerae* L10-48 belonged to the ST type of 884. Remarkably, *V. cholerae* 7-6-5, L1-1, and B5-86 strains were novel ST types, matching none of any known STs.

3.9. Phylogenetic Relatedness of the Four *V. cholerae* Isolates from the Common Freshwater Fish

To further investigate the phylogenetic relatedness of the four *V. cholerae* isolates originating in common freshwater fish, we constructed a phylogenetic tree together with the other 67 *V. cholerae* genomes (Figure 5). Among the 67 *V. cholerae* strains of serotypes O1/O139, and non O1/O139, 32 were isolated from humans, 12 from the environment, 11 from shrimp, 9 from pork, 2 from chicken, and 1 from crab samples between 1962 and 2019 in Asia, Africa, and the USA. This analysis revealed four distinct clusters, designated as Clusters A to D (Table S2).

V. cholerae 7-6-5 (SRA submission no: SAMN37882014) isolated from *A. nobilis* was classified into Cluster A and showed the closest evolutionary distance to *V. cholerae* Vc401 (GenBank accession no: GCA_0016456995.1) isolated from shrimp in 2015 in China. *V. cholerae* L10-48 (SRA submission no: SAMN37882015) isolated from *A. nobilis* was also grouped into Cluster A, but it had the closest distance to *V. cholerae* Vc306 (GenBank assembly accession no: GCA_016456645.1) isolated from pork in 2015 in China. Interestingly, *V. cholerae* B5-86 (SRA submission no: SAMN37882017) isolated from *P. pekinensis* was classified into Cluster D, phylogenetically closest to *V. cholerae* BD18 (GenBank assembly accession no: GCA_03348365.1) isolated from the environment in 2013 in Bangladesh.

Additionally, the evolutionary distance between *V. cholerae* L1-1 (SRA submission no: SAMN37882016) isolated from *C. idellus* and *V. cholerae* BD06 (GenBank assembly accession no: GCA_003348715.1) isolated from the environment in 2013 in Bangladesh was the closest, both of which were classified into Cluster B. Notably, the majority ($n = 27$) of O1/O139 *V. cholerae* isolates from human clinical samples fell into Cluster B.

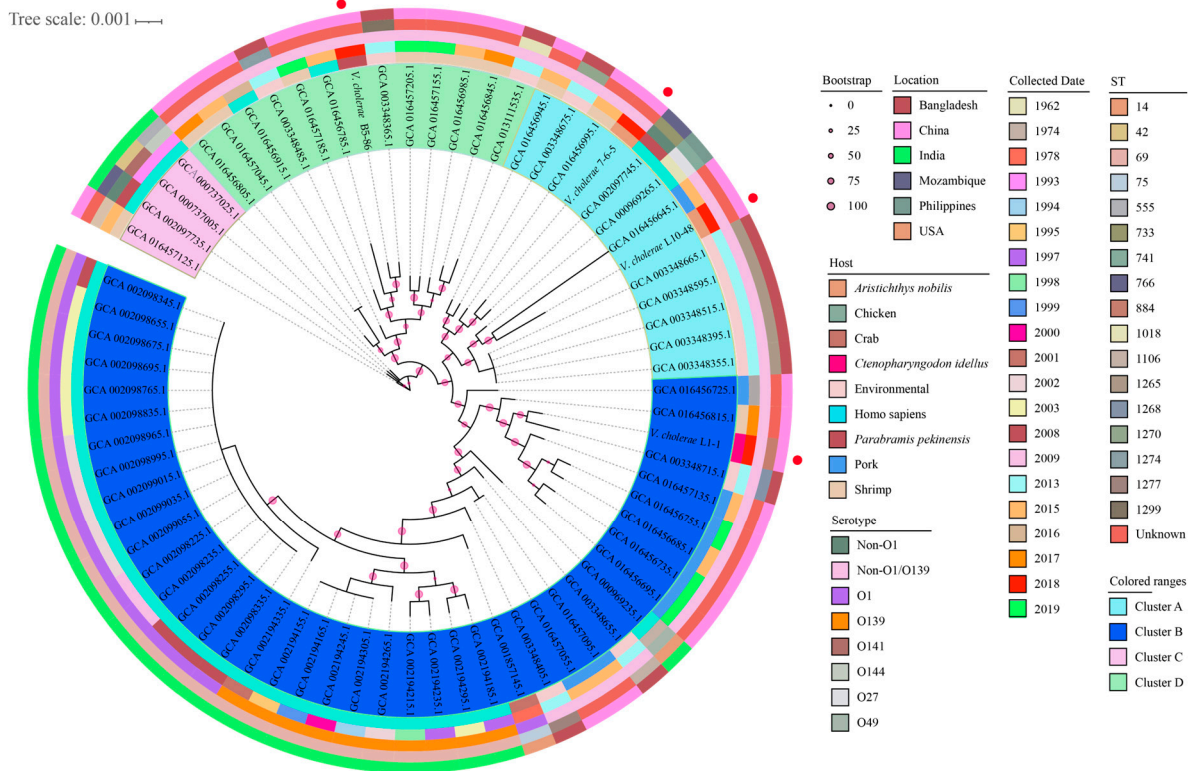


Figure 5. The phylogenetic tree showing the relationship of the 71 *V. cholerae* genomes. The genome sequences of the four *V. cholerae* isolates determined in this study were marked with red dots. The second to the sixth circles represent the host, collected date, serotypes, STs, and location, respectively.

These results indicated the genome diversity of *V. cholerae* isolates from the common freshwater fish and the possible transmission of *V. cholerae* across the national geographic (e.g., Bangladesh and China) and animal species (e.g., fish, shrimp, and pork) boundaries.

The freshwater fish had been tested for the presence of *V. cholerae* in three surveys of our previous research, by which a number of *V. cholerae* strains were isolated and identified [2,13,14]. Of these, enterobacterial repetitive intergenic consensus-polymerase chain reaction (ERIC-PCR)-based fingerprinting of the *V. cholerae* isolates ($n = 400$, 100 from each of four species, e.g., *A. nobilis*, *C. idellus*, and *P. pekinensis*) revealed 328 ERIC-genotypes, which demonstrated a large degree of genomic variation among the isolates [2]. The results in this study provided genome-level evidence of *V. cholerae*'s diversity in freshwater fish.

4. Conclusions

We previously reported that *V. cholerae* was found in freshwater fish such as *A. nobilis*, *C. idellus*, and *P. pekinensis*. In this study, we firstly characterized the growth and genome features of *V. cholerae* isolates with different resistance phenotypes from commonly consumed freshwater fish. The results revealed that the non-O1/O139 *V. cholerae* isolates ($n = 4$) were halophilic and grew optimally at 2% NaCl and pH 8.0 in the TSB medium at 37 °C. *V. cholerae* 7-6-5 from *A. nobilis* had the best fit to the broader spectrum of pH (6.5–8.5) and NaCl (0.5–3.0%) conditions among the isolates.

The draft genome sequences of the four *V. cholerae* isolates were 3.89 Mb–4.15 Mb with an average GC content of 47.35–47.63%. Approximately 3366–3561 genes were predicted to

encode proteins, but 14.9–17.3% of them were of an unknown function. A number of strain-specific genes ($n = 221$ – 311) were found in the four *V. cholerae* isolates, 3 of which belonged to none of any of the known STs. Several putative MGEs existed in the *V. cholerae* isolates, including GIs ($n = 4$ – 9), prophages ($n = 0$ – 3), Ins ($n = 1$ – 1), and ISs ($n = 0$ – 3). Notably, CRISPR-Cas system arrays ($n = 2$ – 10) were found in the *V. cholerae* genomes, whereby the potential immunity defense system could be active. Comparative genomic analyses also revealed many putative virulence-associated genes ($n = 106$ – 122) and antibiotic resistance-related genes ($n = 4$ – 5), suggesting a potential risk of consuming the aquatic products contaminated by these *V. cholerae* isolates.

Taken together, the results of this study demonstrated the bacterial broader-spectrum growth traits and fill prior gaps of knowledge in the genomes of *V. cholerae* from freshwater fish. This study should be useful for the future investigation of the evolution of the waterborne pathogen worldwide.

Supplementary Materials: The following supporting information can be downloaded at <https://www.mdpi.com/article/10.3390/d16050268/s1>. Table S1: The phenotypes of the four *V. cholerae* isolates used in this study; Table S2: The seventy-one *V. cholerae* strains with genome sequences used in the phylogenetic tree; Table S3: The identified repeats in the four *V. cholerae* genomes; Table S4: The identified GIs in the four *V. cholerae* genomes; Table S5: The identified prophage gene clusters in the four *V. cholerae* genomes; Table S6: The identified Ins in the four *V. cholerae* genomes; Table S7: The identified ISs in the four *V. cholerae* genomes; Table S8: The identified CRISPR-Cas arrays in the four *V. cholerae* genomes; Table S9: The potential virulence factor-encoding genes identified in the four *V. cholerae* genomes [58–64]; Figure S1: The gene function of the GIs identified in the four *V. cholerae* genomes. Different colors refer to COG classification to mark gene function and genes not annotated to the COG database are displayed in grey. (A–D): the *V. cholerae* 7-6-5, L10-48, L1-1, and B5-86 genomes, respectively; Figure S2: The k-mer analysis for the four *V. cholerae* subread data based on the number of unique 17-mers. (A–D): the *V. cholerae* 7-6-5, L10-48, L1-1, and B5-86 genomes, respectively; Figure S3: Gene organizations of the GIs identified in the four *V. cholerae* genomes. Different colors refer to COG classification in Figure S1; Figure S4: The structure diagram of the prophage gene clusters identified in the four *V. cholerae* genomes; Figure S5: The structure diagram of the Ins identified in the four *V. cholerae* genomes; Figure S6: The structural features of the CRISPR arrays identified in the four *V. cholerae* genomes. The repeat sequences are shown by the rectangle of different colors and the spacer regions are represented by rhombuses of different colors.

Author Contributions: X.Q.: investigation, data curation, and writing—original draft preparation; L.Y.: investigation; Y.X.: data analysis; L.X. and Y.W.: supervision and discussion; L.C.: funding acquisition, conceptualization, and writing—review and editing. All authors have read and agreed to the published version of the manuscript.

Funding: This study was supported by Science and Technology Commission of Shanghai Municipality, grant number 17050502200.

Institutional Review Board Statement: Not applicable.

Data Availability Statement: Draft genome sequences of the four *V. cholerae* isolates were deposited in the GenBank database under the bioSample accession numbers SAMN37882014, SAMN37882015, SAMN37882016, and SAMN37882017, respectively.

Acknowledgments: The authors are grateful to Huiqiong Guan and Suo Sun at Shanghai Ocean University for their help in the data analyses.

Conflicts of Interest: The authors declare no conflicts of interest.

References

1. Montero, D.A.; Vidal, R.M.; Velasco, J.; George, S.; Lucero, Y.; Gómez, L.A.; Carreño, L.J.; García-Betancourt, R.; O’Ryan, M. *Vibrio cholerae*, classification, pathogenesis, immune response, and trends in vaccine development. *Front. Med.* **2023**, *10*, 1155751. [[CrossRef](#)] [[PubMed](#)]
2. Xu, M.; Wu, J.; Chen, L. Virulence, antimicrobial and heavy metal tolerance, and genetic diversity of *Vibrio cholerae* recovered from commonly consumed freshwater fish. *Environ. Sci. Pollut. Res. Int.* **2019**, *26*, 27338–27352. [[CrossRef](#)] [[PubMed](#)]

3. Waldor, M.K.; Mekalanos, J.J. Lysogenic conversion by a filamentous phage encoding cholera toxin. *Science* **1996**, *272*, 1910–1914. [[CrossRef](#)] [[PubMed](#)]
4. Almansour, A.M.; Alhadlaq, M.A.; Alzahrani, K.O.; Mukhtar, L.E.; Alharbi, A.L.; Alajel, S.M. The silent threat: Antimicrobial-resistant pathogens in food-producing animals and their impact on public health. *Microorganisms* **2023**, *11*, 2127. [[CrossRef](#)]
5. Taviani, E.; van den Berg, H.; Nhassengo, F.; Ngulube, E.; Paulo, J.; Pedro, O.; Ferrero, G. Occurrence of waterborne pathogens and antibiotic resistance in water supply systems in a small town in Mozambique. *BMC Microbiol.* **2022**, *22*, 243. [[CrossRef](#)] [[PubMed](#)]
6. Abioye, O.E.; Nontongana, N.; Osunla, C.A.; Okoh, A.I. Antibiotic resistance and virulence genes profiling of *Vibrio cholerae* and *Vibrio mimicus* isolates from some seafood collected at the aquatic environment and wet markets in Eastern Cape Province, South Africa. *PLoS ONE* **2023**, *18*, e0290356. [[CrossRef](#)] [[PubMed](#)]
7. Schmidt, K.; Scholz, H.C.; Appelt, S.; Michel, J.; Jacob, D.; Dupke, S. Virulence and resistance patterns of *Vibrio cholerae* non-O1/non-O139 acquired in Germany and other European countries. *Front. Microbiol.* **2023**, *14*, 1282135. [[CrossRef](#)] [[PubMed](#)]
8. Arnold, B.J.; Huang, I.T.; Hanage, W.P. Horizontal gene transfer and adaptive evolution in bacteria. *Nat. Rev. Microbiol.* **2022**, *20*, 206–218. [[CrossRef](#)] [[PubMed](#)]
9. Sun, S.; Gu, T.; Ou, Y.; Wang, Y.; Xie, L.; Chen, L. Environmental compatibility and genome flexibility of *Klebsiella oxytoca* isolated from eight species of aquatic animals. *Diversity* **2024**, *16*, 30. [[CrossRef](#)]
10. Haudiquet, M.; Sousa, J.M.; Touchon, M.; Rocha, E.P.C. Selfish, promiscuous and sometimes useful: How mobile genetic elements drive horizontal gene transfer in microbial populations. *Philos. Trans. R. Soc. Lond. B Biol. Sci.* **2022**, *377*, 20210234. [[CrossRef](#)]
11. Dorado, G.; Gálvez, S.; Rosales, T.E.; Vásquez, V.F.; Hernández, P. Analyzing modern biomolecules: The revolution of nucleic-acid sequencing—Review. *Biomolecules* **2021**, *11*, 1111. [[CrossRef](#)] [[PubMed](#)]
12. Evrony, G.D.; Hinch, A.G.; Luo, C. Applications of single-cell DNA sequencing. *Annu. Rev. Genom. Hum. G.* **2021**, *22*, 171–197. [[CrossRef](#)] [[PubMed](#)]
13. Chen, D.; Li, X.; Ni, L.; Xu, D.; Xu, Y.; Ding, Y.; Xie, L.; Chen, L. First experimental evidence for the presence of potentially toxic *Vibrio cholerae* in snails, and virulence, cross-resistance and genetic diversity of the bacterium in 36 species of aquatic food animals. *Antibiotics* **2021**, *10*, 412. [[CrossRef](#)] [[PubMed](#)]
14. Fu, H.; Yu, P.; Liang, W.; Kan, B.; Peng, X.; Chen, L. Virulence, resistance, and genomic fingerprint traits of *Vibrio cholerae* isolated from 12 species of aquatic products in Shanghai, China. *Microb. Drug. Resist.* **2020**, *26*, 1526–1539. [[CrossRef](#)] [[PubMed](#)]
15. Song, Y.; Yu, P.; Li, B.; Pan, Y.; Zhang, X.; Cong, J.; Zhao, Y.; Wang, H.; Chen, L. The mosaic accessory gene structures of the SXT/R391-like integrative and conjugative elements derived from *Vibrio* spp. isolated from aquatic products and environment in the Yangtze River Estuary, China. *BMC Microbiol.* **2013**, *13*, 214. [[CrossRef](#)]
16. Miller, C.J.; Drasar, B.S.; Feachem, R.G. Response of toxigenic *Vibrio cholerae* O1 to physico-chemical stresses in aquatic environments. *J. Hygiene.* **1984**, *93*, 475–495. [[CrossRef](#)] [[PubMed](#)]
17. Guan, H.; Xie, L.; Chen, L. Survival and genome evolution signatures of *Klebsiella pneumoniae* isolates originated in seven species of aquatic animals. *Diversity* **2023**, *15*, 527. [[CrossRef](#)]
18. Xu, D.; Peng, X.; Xie, L.; Chen, L. Survival and genome diversity of *Vibrio parahaemolyticus* isolated from edible aquatic animals. *Diversity* **2022**, *14*, 350. [[CrossRef](#)]
19. Yu, P.; Yang, L.; Wang, J.; Su, C.; Qin, S.; Zeng, C.; Chen, L. Genomic and transcriptomic analysis reveal multiple strategies for the cadmium tolerance in *Vibrio parahaemolyticus* N10-18 isolated from aquatic animal *Ostrea Gigas Thunberg*. *Foods* **2022**, *11*, 3777. [[CrossRef](#)] [[PubMed](#)]
20. Luo, R.; Liu, B.; Xie, Y.; Li, Z.; Huang, W.; Yuan, J.; He, G.; Chen, Y.; Pan, Q.; Liu, Y.; et al. SOAPdenovo2: An empirically improved memory-efficient short-read de novo assembler. *GigaScience* **2012**, *1*, 18. [[CrossRef](#)]
21. Delcher, A.L.; Bratke, K.A.; Powers, E.C.; Salzberg, S.L. Identifying bacterial genes and endosymbiont DNA with Glimmer. *Bioinformatics* **2007**, *23*, 673–679. [[CrossRef](#)] [[PubMed](#)]
22. Chan, P.P.; Lowe, T.M. tRNAscan-SE: Searching for tRNA genes in genomic sequences. *Methods Mol. Biol.* **2019**, *1962*, 1–14. [[CrossRef](#)]
23. Pal, C.; Bengtsson-Palme, J.; Rensing, C.; Kristiansson, E.; Larsson, D.G.J. BacMet: Antibacterial biocide and metal resistance genes database. *Nucleic. Acids. Res.* **2014**, *42*, D737–D743. [[CrossRef](#)] [[PubMed](#)]
24. Bertelli, C.; Fiona, S.L. Improved genomic island predictions with IslandPath-DIMOB. *Bioinformatics* **2018**, *34*, 2161–2167. [[CrossRef](#)]
25. Fouts, D.E. Phage_Finder: Automated identification and classification of prophage regions in complete bacterial genome sequences. *Nucleic. Acids. Res.* **2006**, *34*, 5839–5851. [[CrossRef](#)]
26. Cury, J.; Jové, T.; Touchon, M.; Néron, B.; Rocha, E.P. Identification and analysis of integrons and cassette arrays in bacterial genomes. *Nucleic. Acids. Res.* **2016**, *44*, 4539–4550. [[CrossRef](#)]
27. Siguier, P.; Perochon, J.; Lestrade, L.; Mahillon, J.; Chandler, M. ISfinder: The reference centre for bacterial insertion sequences. *Nucleic. Acids. Res.* **2006**, *34*, D32–D36. [[CrossRef](#)]
28. Bland, C.; Ramsey, T.L.; Sabree, F.; Lowe, M.; Brown, K.; Kyrpides, N.C.; Hugenholtz, P. CRISPR recognition tool (CRT): A tool for automatic detection of clustered regularly interspaced palindromic repeats. *BMC Bioinform.* **2007**, *8*, 209. [[CrossRef](#)] [[PubMed](#)]
29. Li, L.; Stoeckert, C.J., Jr.; Roos, D.S. OrthoMCL: Identification of ortholog groups for eukaryotic genomes. *Genome. Res.* **2003**, *13*, 2178–2189. [[CrossRef](#)]

30. Jolley, K.A.; Bray, J.E.; Maiden, M.C.J. Open-access bacterial population genomics: BIGSdb software, the PubMLST.org website and their applications. *Wellcome. Open. Res.* **2018**, *3*, 124. [[CrossRef](#)]
31. Heidelberg, J.F.; Eisen, J.A.; Nelson, W.C.; Clayton, R.A.; Gwinn, M.L.; Dodson, R.J.; Haft, D.H.; Hickey, E.K.; Peterson, J.D.; Umayam, L.; et al. DNA sequence of both chromosomes of the cholera pathogen *Vibrio cholerae*. *Nature* **2000**, *406*, 477–483. [[CrossRef](#)] [[PubMed](#)]
32. McKerral, J.C.; Papudeshi, B.; Inglis, L.K.; Roach, M.J.; Decewicz, P.; McNair, K.; Luque, A.; Dinsdale, E.A.; Edwards, R.A. The promise and pitfalls of prophages. *bioRxiv* **2023**. bioRxiv: 537752. [[CrossRef](#)] [[PubMed](#)]
33. An, X.L.; Chen, Q.L.; Zhu, D.; Zhu, Y.G.; Gillings, M.R.; Su, J.Q. Impact of wastewater treatment on the prevalence of integrons and the genetic diversity of integron gene cassettes. *Appl. Environ. Microb.* **2018**, *84*, e02766-17. [[CrossRef](#)] [[PubMed](#)]
34. Sabbagh, P.; Rajabnia, M.; Maali, A.; Ferdosi-Shahandashti, E. Integron and its role in antimicrobial resistance: A literature review on some bacterial pathogens. *Iran. J. Basic. Med. Sci.* **2021**, *24*, 136–142. [[CrossRef](#)] [[PubMed](#)]
35. Gonçalves, O.S.; Campos, K.F.; Assis, J.C.S.; Fernandes, A.S.; Souza, T.S.; Rodrigues, L.G.C.; Queiroz, M.V.; Santana, M.F. Transposable elements contribute to the genome plasticity of *Ralstonia solanacearum* species complex. *Microb. Genom.* **2020**, *6*, e000374. [[CrossRef](#)]
36. Zakrzewska, M.; Burmistrz, M. Mechanisms regulating the CRISPR-Cas systems. *Front. Microbiol.* **2023**, *14*, 1060337. [[CrossRef](#)] [[PubMed](#)]
37. Deveau, H.; Garneau, J.E.; Moineau, S. CRISPR/Cas system and its role in phage-bacteria interactions. *Annu. Rev. Microbiol.* **2010**, *64*, 475–493. [[CrossRef](#)] [[PubMed](#)]
38. Wang, P.; Du, X.; Zhao, Y.; Wang, W.; Cai, T.; Tang, K.; Wang, X. Combining CRISPR/Cas9 and natural excision for the precise and complete removal of mobile genetic elements in bacteria. *Appl. Environ. Microbiol.* **2024**, *90*, e0009524. [[CrossRef](#)]
39. Austin, B. Vibrios as causal agents of zoonoses. *Vet. Microbiol.* **2010**, *140*, 310–317. [[CrossRef](#)]
40. Ceccarelli, D.; Chen, A.; Hasan, N.A.; Rashed, S.M.; Huq, A.; Colwell, R.R. Non-O1/non-O139 *Vibrio cholerae* carrying multiple virulence factors and *V. cholerae* O1 in the Chesapeake Bay, Maryland. *Appl. Environ. Microbiol.* **2015**, *81*, 1909–1918. [[CrossRef](#)]
41. Lee, A.; White, N.; Walle, C.F. The intestinal zonula occludens toxin (ZOT) receptor recognises non-native ZOT conformers and localises to the intercellular contacts. *FEBS Lett.* **2003**, *555*, 638–642. [[CrossRef](#)] [[PubMed](#)]
42. Dong, T.G.; Ho, B.T.; Yoder-Himes, D.R.; Mekalanos, J.J. Identification of T6SS-dependent effector and immunity proteins by Tn-seq in *Vibrio cholerae*. *Proc. Natl. Acad. Sci. USA* **2013**, *110*, 2623–2628. [[CrossRef](#)] [[PubMed](#)]
43. Kodama, T.; Rokuda, M.; Park, K.S.; Cantarelli, V.V.; Matsuda, S.; Iida, T.; Honda, T. Identification and characterization of VopT, a novel ADP-ribosyltransferase effector protein secreted via the *Vibrio parahaemolyticus* type III secretion system 2. *Cell. Microbiol.* **2007**, *9*, 2598–2609. [[CrossRef](#)] [[PubMed](#)]
44. Sun, Y.; Wang, X.; Li, J.; Xue, F.; Tang, F.; Dai, J. Extraintestinal pathogenic *Escherichia coli* utilizes the surface-expressed elongation factor Tu to bind and acquire iron from holo-transferrin. *Virulence* **2022**, *13*, 698–713. [[CrossRef](#)] [[PubMed](#)]
45. Inzana, T.J. The many facets of lipooligosaccharide as a virulence factor for *Histophilus somni*. *Curr. Top. Microbiol. Immunol.* **2016**, *396*, 131–148. [[PubMed](#)]
46. Sheahan, K.L.; Cordero, C.L.; Satchell, K.J. Identification of a domain within the multifunctional *Vibrio cholerae* RTX toxin that covalently cross-links actin. *Proc. Natl. Acad. Sci. USA* **2004**, *101*, 9798–9803. [[CrossRef](#)] [[PubMed](#)]
47. De, S.; Olson, R. Crystal structure of the *Vibrio cholerae* cytolysin heptamer reveals common features among disparate pore-forming toxins. *Proc. Natl. Acad. Sci. USA* **2011**, *108*, 7385–7390. [[CrossRef](#)]
48. Nishino, K.; Senda, Y.; Yamaguchi, A. CRP regulator modulates multidrug resistance of *Escherichia coli* by repressing the mdtEF multidrug efflux genes. *J. Antibiot.* **2008**, *61*, 120–127. [[CrossRef](#)] [[PubMed](#)]
49. Henderson, J.C.; Herrera, C.M.; Trent, M.S. AlmG, responsible for polymyxin resistance in pandemic *Vibrio cholerae*, is a glycoltransferase distantly related to lipid A late acyltransferases. *J. Biol. Chem.* **2017**, *292*, 21205–21215. [[CrossRef](#)]
50. Tacão, M.; Moura, A.; Correia, A.; Henriques, I. Co-resistance to different classes of antibiotics among ESBL-producers from aquatic systems. *Water Res.* **2014**, *48*, 100–107. [[CrossRef](#)]
51. Lin, H.V.; Massam-Wu, T.; Lin, C.P.; Wang, Y.A.; Shen, Y.; Lu, W.; Hsu, P.; Chen, Y.; Borges-Walmsley, M.I.; Walmsley, A.R. The *Vibrio cholerae* var regulon encodes a metallo- β -lactamase and an antibiotic efflux pump, which are regulated by VarR, a LysR-type transcription factor. *PLoS ONE* **2017**, *12*, e0184255. [[CrossRef](#)] [[PubMed](#)]
52. Lepuschitz, S.; Baron, S.; Larvor, E.; Granier, S.A.; Pretzer, C.; Mach, R.L.; Farnleitner, A.H.; Ruppitsch, W.; Pleininger, S.; Indra, A.; et al. Phenotypic and genotypic antimicrobial resistance traits of *Vibrio cholerae* non-O1/non-O139 isolated from a large Austrian lake frequently associated with cases of human infection. *Front. Microbiol.* **2019**, *10*, 2600. [[CrossRef](#)]
53. Melano, R.; Petroni, A.; Garutti, A.; Saka, H.A.; Mange, L.; Pasterán, F.; Rapoport, M.; Rossi, A.; Galas, M. New carbenicillin-hydrolyzing β -lactamase (CARB-7) from *Vibrio cholerae* non-O1, non-O139 strains encoded by the VCR region of the *V. cholerae* genome. *Antimicrob. Agents Chemother.* **2002**, *46*, 2162–2168. [[CrossRef](#)] [[PubMed](#)]
54. Lacour, S.; Bechet, E.; Cozzone, A.J.; Mijakovic, I.; Grangeasse, C. Tyrosine phosphorylation of the UDP-glucose dehydrogenase of *Escherichia coli* is at the crossroads of colanic acid synthesis and polymyxin resistance. *PLoS ONE* **2008**, *3*, e3053. [[CrossRef](#)] [[PubMed](#)]
55. Bonifer, C.; Glaubitz, C. MsbA: An ABC transporter paradigm. *Biochem. Soc. Trans.* **2021**, *49*, 2917–2927. [[CrossRef](#)] [[PubMed](#)]

56. Siddi, G.; Piras, F.; Meloni, M.P.; Gyomoese, P.; Torpdahl, M.; Fredriksson-Ahomaa, M.; Migoni, M.; Cabras, D.; Cuccu, M.; De Santis, E.P.L.; et al. Hunted wild boars in sardinia: Prevalence, antimicrobial resistance and genomic analysis of *Salmonella* and *Yersinia enterocolitica*. *Foods* **2023**, *13*, 65. [[CrossRef](#)] [[PubMed](#)]
57. Nguyen, T.H.T.; Nguyen, H.D.; Le, M.H.; Nguyen, T.T.H.; Nguyen, T.D.; Nguyen, D.L.; Nguyen, Q.H.; Nguyen, T.K.O.; Michalet, S.; Dijoux-Franca, M.; et al. Efflux pump inhibitors in controlling antibiotic resistance: Outlook under a heavy metal contamination context. *Molecules* **2023**, *28*, 2912. [[CrossRef](#)] [[PubMed](#)]
58. Syed, K.A.; Beyhan, S.; Correa, N.; Queen, J.; Liu, J.; Peng, F.; Satchell, K.J.F. Yildiz, F.; Klose, K.E. The *Vibrio cholerae* flagellar regulatory hierarchy controls expression of virulence factors. *J. Bacteriol.* **2009**, *191*, 6555–6570. [[CrossRef](#)] [[PubMed](#)]
59. Utada, A.S.; Bennett, R.R.; Fong, J.C.N.; Gibiansky, M.L.; Yildiz, F.H.; Golestanian, R.; Wong, G.C.L. *Vibrio cholerae* use pili and flagella synergistically to effect motility switching and conditional surface attachment. *Nat. Commun.* **2014**, *5*, 4913. [[CrossRef](#)]
60. Chen, X.; Schauder, S.; Potier, N.; Dorsselaer, A.V.; Pelczer, I.; Bassler, B.L.; Hughson, F.M. Structural identification of a bacterial quorum-sensing signal containing boron. *Nature*. **2002**, *415*, 545–549. [[CrossRef](#)]
61. Chen, L.; Yang, J.; Yu, J.; Yao, Z.; Sun, L.; Shen, Y.; Jin, Q. VFDB: A reference database for bacterial virulence factors. *Nucleic. Acids. Res.* **2005**, *33*, D325–D328. [[CrossRef](#)] [[PubMed](#)]
62. Lee, N.Y.; Lee, H.Y.; Lee, K.H.; Han, S.H.; Park, S.J. *Vibrio vulnificus* IlpA induces MAPK-mediated cytokine production via TLR1/2 activation in THP-1 cells, a human monocytic cell line. *Mol. Immunol.* **2011**, *49*, 143–154. [[CrossRef](#)] [[PubMed](#)]
63. Fullner, K.J.; Mekalanos, J.J. In vivo covalent cross-linking of cellular actin by the *Vibrio cholerae* RTX toxin. *EMBO J.* **2000**, *19*, 5315–5323. [[CrossRef](#)]
64. Higgins, D.A.; Pomianek, M.E.; Kraml, C.M.; Taylor, R.K.; Semmelhack, M.F.; Bassler, B.L. The major *Vibrio cholerae* autoinducer and its role in virulence factor production. *Nature* **2007**, *450*, 883–886. [[CrossRef](#)] [[PubMed](#)]

Disclaimer/Publisher’s Note: The statements, opinions and data contained in all publications are solely those of the individual author(s) and contributor(s) and not of MDPI and/or the editor(s). MDPI and/or the editor(s) disclaim responsibility for any injury to people or property resulting from any ideas, methods, instructions or products referred to in the content.